

THE STUDY OF GALACTIC BEAT CEPHEIDS WITH APPLICATION OF ITS RESULTS TO THOSE IN THE MAGELLANIC CLOUDS

F. A. Chekhonadskikh, V. V. Kovtyukh, S. I. Belik
Astronomical observatory of Odessa National University,
Odessa, Ukraine, *chehonadskih@gmail.com*

ABSTRACT. A thorough study of the correlation between P_1/P_0 ratio, fundamental period, and chemical composition (abundances of metals that compose Z) was conducted to investigate the significance of the iron-peak elements on the ratio. The results suggested a more accurate P_1/P_0 ratio that can be useful as an alternative means of determining a beat Cepheid's metallicity. Metallicities for a large sample of stars were analysed using the suggested ratio. The metallicity distribution function for the Magellanic Clouds projected on the celestial sphere was constructed for the first time, and several stars with anomalous metallicities were detected. The average metallicities of the Magellanic Clouds were also obtained independently: -0.30 dex for the Large Magellanic Cloud (LMC) and -0.49 dex for the Small Magellanic Cloud (SMC). The $[Fe/H]$ values for two newly-found bimodal Cepheids in the Galactic bulge were estimated: -0.39 dex for OGLE-BLG-CEP-03 and -0.29 dex for OGLE-BLG-CEP-21.

Key words: stars: Classical Cepheids – stars: abundance, metallicity

1. Introduction

In recent years the beat Cepheids have often been called double-mode Cepheids or bimodal Cepheids. They imply the same objects in any case: such Cepheids pulsate in two radial modes simultaneously. There can be different combinations of two pulsation modes for a bimodal Cepheid, as implied by their period ratios, such as first overtone and fundamental mode (P_1/P_0), or second and first overtone modes (P_2/P_1), or even third and first overtone modes (P_3/P_1). Exotic Cepheids implied by the last type were found only in other galaxies, such as the huge number discovered in the OGLE project surveys (see Udalski et al., 2008). There is a small sample of bimodal Cepheids in our Galaxy, their total number does not exceed 25 and the majority of them are P_1/P_0 pulsators.

It is well-known that the P_1/P_0 period ratio for bimodal Cepheids strongly depends on the physical parameters of the stars, such as mass (M), luminosity (L), mean effective temperature (T_{eff}), and metallicity (Z). The metallicity Z is an additive measure comprised of all elements heavier than helium. But it is not yet known which elements have greater significance with regard to P_1/P_0 ratio.

According to some theoretical studies we might assume that such elements could be the iron-peak elements, some researchers have suggested the importance of the P_1/P_0 – $[Fe/H]$ relation (see Sziládi et al., 2007). To date it has not been possible to carry out an in-depth statistical analysis regarding the influence of other elements on the indicated relationship. The results of such an analysis are presented here. We expanded the applicability of the suggested relation through our sample of beat Cepheids enlarged by the addition of the metal-deficient Cepheid V371 Per. It enabled us to conduct an in-depth study of the metallicity distribution in the Magellanic Clouds where metallicities are lower than in our Galaxy.

2. The spectral material

High signal-to-noise spectra were obtained using the 2.2-m MPG telescope and FEROS spectrograph at ESO La Silla (Chile). The spectra cover a continuous wavelength range from 4000 to 7850 Å with a resolving power of about 48 000. Typical maximum S/N values (per pixel) for the spectra exceeded 150 (see Table 1).

A broad-lined B-star with a S/N ratio exceeding that of the program stars was observed nightly to make the telluric line cancellation possible when necessary. Table 2 also contains some details of the program Cepheid observations. Previously, the spectra were used only to determine the $[Fe/H]$ abundance (Sziládi et al. 2007).

Further processing, such as continuum placement, line depth and equivalent width (R_λ and EW) calculations were carried out using the DECH20 software

Table 1: Atmospheric parameters of the program stars

Star	MJD	S/N	T_{eff} (K)	$\log g$ (dex)	V_t (km s^{-1})
Y Car	53155.953274	187	5890	2.2	3.0
	53158.133919	270	6564	2.0	3.7
GZ Car	53158.077868	125	5904	2.1	4.4
EY Car	53156.081982	142	6000	2.6	4.5
	53158.051978	139	5855	2.1	3.6
V701 Car	53156.031049	169	5755	2.0	3.0
BK Cen	53156.135605	201	5866	2.2	3.8
	53158.211729	151	5830	2.1	3.1
UZ Cen	53156.163756	210	6307	2.3	4.0
	53158.154992	168	5809	2.1	3.5
V1210 Cen	53158.181235	274	5868	2.1	4.2
VX Pup	53157.943348	274	6415	2.6	3.8
EW Sct	53156.311619	150	5668	1.9	3.7
	53157.437109	197	5985	2.2	4.6
	53158.416900	228	6383	2.4	4.3
V367 Sct	53156.358955	151	6111	2.3	4.7
	53157.387011	146	6212	2.2	4.8
V458 Sct	53156.258363	218	6160	2.2	4.5
	53157.311805	183	5984	2.0	3.5
BQ Ser	53156.285838	133	5835	2.0	3.8
	53157.412207	139	6210	2.1	3.9
	53158.389508	169	6143	2.2	4.0
U TrA	53156.229253	300	5909	2.1	3.8
	53158.290333	270	6054	2.4	3.8
AP Vel	53155.970338	126	5855	2.1	4.0
	53158.010053	154	5970	2.4	4.0
AX Vel	53155.993418	328	6241	2.3	3.5
	53158.035784	232	6205	2.1	3.6

package by Galazutdinov (1992). The EWs were measured by the Gaussian fitting.

3. Fundamental parameters and chemical composition

To determine the effective temperatures (T_{eff}) for our stars, we employed the line-depth ratio method developed by Kovtyukh (2007). The technique enabled us to determine T_{eff} with an exceptional accuracy. It is based on the ratio of the central depths of two lines that differ markedly in their functional dependence on T_{eff} (and there are a few tens of line pairs that were used in the analysis). The method is independent of interstellar reddening and just marginally dependent on individual characteristics of the stars, such as rotation, microturbulence, metallicity, etc. With ~ 50 – 70 calibrations per spectrum the uncertainty was 10–20K for spectra with S/N ratio greater than 100 and 30–50 K for those with S/N ratio less than 100.

To determine the microturbulent velocities (V_t) and gravities ($\log g$), we used a modified method of standard analysis proposed by Kovtyukh & Andrievsky (1999). The method implies that V_t is determined from the Fe II lines (instead of the Fe I lines used in classical abundance analyses). The value of $\log g$ is determined by forcing the equality of the total iron abundance derived from the Fe I and Fe II lines. Normally, the iron abundance determined from the Fe I line using this method appears to exhibit a strong dependence on EW (because of non-LTE effects). In that case, the abundance extrapolated to zero EW is considered to be the true value.

Table 2: The Galactic beat Cepheids parameters

Star	Sp	P_1/P_0	[Fe/H] (dex)	R_G (kpc)
Y Car	1	0.7032	0.02	7.67
EY Car	2	0.7079	0.07	7.52
GZ Car	1	0.7054	0.00	7.63
V701 Car	2	0.7017	0.07	7.72
TU Cas	12	0.7097	0.03	8.31
UZ Cen	2	0.7064	−0.02	7.45
BK Cen	2	0.7004	0.12	7.24
1210 Cen	1	0.7035	0.08	6.39
V371 Per	2	0.7312	−0.42	10.61
VX Pup	2	0.7104	−0.06	8.64
EW Sct	6	0.6986	0.04	7.57
V367 Sct	3	0.6968	0.05	6.43
V458 Sct	2	0.6993	0.09	6.92
BQ Ser	6	0.7052	−0.04	7.17
U TrA	2	0.7105	−0.07	7.14
AP Vel	2	0.7033	0.06	8.24
AX Vel	3	0.7059	−0.05	8.11

Remarks: Sp – number of used spectra;

R_G – Galactocentric distance ($R_{G,\odot} = 7.9$ kpc)

The physical parameters of the program stars are presented in Table 1. The elemental abundances were computed using the Kurucz WIDTH9 code. As usual, the abundance values are given relative to the solar values, which were adopted from Grevesse et al. (1996). Moreover, we used the chemical composition determined for V371 Per by Kovtyukh et al. (2012) and for TU Cas by Andrievsky et al. (2002); we also used abundances determined from additional spectra of EW Sct and BQ Ser. The combined data are given in Tables 2 and 3.

4. Correlation analysis of Z components

As there was a sample of 17 program stars available, we could only identify the impact of 15 external factors from regression analysis. As ensues from observations, the P_1/P_0 ratio depends on the fundamental period P_0 itself. In addition, we attempted to separate the effects of metallicity and accounted for that in the relation. From such considerations we constructed the relationship as a linear model that, apart from period P_0 , contains abundances of 14 chemical elements found in stellar atmospheres. There were several α -elements, the iron-peak and other elements, for which $A(\text{El}) > 7$ dex. Regression and correlation analyses for the constructed model were carried out, and quite predictable results were obtained.

Oxygen is the most common element after hydrogen and helium. The oxygen abundance in stellar atmospheres $A(\text{O})$ exceeds 8 dex and tends to 9 dex. Values around 7.5 dex are typical for nitrogen, carbon, most

Table 3: Chemical composition of the program stars

Star	C	N	O	Na	Mg	Al	Si	S	Ca	Sc	Ti	V	Cr	Mn
V371 Per	-0.32	-0.21	-0.18	-0.45	-0.43	-0.28	-0.28	-0.13	-0.25	-0.17	-0.07	-0.18	-0.42	-0.41
TU Cas	-0.19	...	-0.03	0.15	-0.19	0.14	0.10	-0.03	-0.02	-0.19	0.05	0.02	0.02	0.06
U TrA	-0.29	0.33	-0.03	0.05	-0.19	0.09	-0.02	0.01	-0.12	-0.10	-0.02	-0.12	-0.15	-0.25
EY Car	-0.26	0.38	0.16	0.06	-0.05	0.31	0.08	0.17	-0.01	0.05	0.04	0.07	0.02	0.01
VX Pup	-0.30	0.20	-0.06	-0.06	-0.22	-0.09	-0.12	0.00	-0.15	-0.15	-0.07	-0.09	-0.10	-0.25
AP Vel	-0.11	0.45	0.11	0.12	-0.03	0.31	0.08	0.19	-0.03	0.04	0.04	-0.02	-0.03	-0.10
BK Cen	-0.09	...	0.08	0.27	-0.03	0.20	0.14	0.25	0.04	0.06	0.12	0.04	0.12	0.02
UZ Cen	-0.25	0.30	-0.04	0.16	-0.15	0.06	-0.01	0.02	-0.08	-0.05	-0.03	-0.16	-0.04	-0.20
Y Car	-0.18	0.25	0.01	0.12	-0.19	0.06	0.04	0.09	0.01	0.00	0.00	-0.07	-0.03	-0.19
AX Vel	-0.28	0.46	-0.06	0.09	-0.06	0.16	0.04	0.08	-0.04	-0.05	-0.04	-0.08	-0.08	-0.23
V701 Car	-0.06	0.36	0.02	0.30	-0.01	0.21	0.10	0.15	0.11	0.06	0.07	-0.02	0.07	-0.03
GZ Car	-0.12	...	-0.16	0.10	-0.13	0.08	0.01	0.11	-0.19	-0.08	0.03	-0.07	-0.11	-0.15
BQ Ser	-0.17	0.27	-0.13	0.10	-0.12	0.18	0.05	0.12	-0.04	-0.10	0.02	-0.03	-0.02	-0.10
V1210 Cen	0.09	0.17	0.13	0.03	-0.06	0.26	0.09	0.26	0.04	0.07	0.09	0.02	0.02	0.00
V458 Sct	-0.17	0.41	-0.11	0.25	-0.07	0.33	0.13	0.21	0.05	0.04	0.12	0.05	0.09	-0.02
EW Sct	-0.04	0.20	-0.01	0.02	-0.12	0.17	0.06	0.16	0.02	-0.05	0.06	0.03	0.04	-0.02
V367 Sct	0.02	0.60	0.06	0.22	0.02	0.34	0.09	0.24	-0.10	0.06	0.09	0.05	-0.02	-0.06

Star	Fe	Co	Ni	Cu	Zn	Y	Zr	La	Ce	Pr	Nd	Sm	Eu	Gd
V371 Per	-0.42	-0.27	-0.34	-0.35	-0.08	0.03	-0.05	-0.02	0.03	-0.24	-0.22	...	0.01	...
TU Cas	0.03	-0.08	-0.04	0.15	0.46	0.17	0.01	0.24	-0.05	...	0.08	...	0.11	0.17
U TrA	-0.07	-0.17	-0.06	-0.06	-0.28	0.06	-0.02	0.09	-0.06	-0.09	-0.03	...	0.05	...
EY Car	0.07	0.14	0.06	0.21	-0.20	0.16	-0.10	0.17	0.12	...	-0.02	...
VX Pup	-0.06	-0.14	-0.11	-0.26	-0.36	0.02	-0.08	0.06	-0.03	-0.15	-0.12	0.18	0.03	...
AP Vel	0.06	-0.05	0.02	0.00	-0.20	0.17	...	0.17	0.01	...	0.10	...	0.12	...
BK Cen	0.12	0.03	0.10	0.09	-0.08	0.25	0.08	0.15	0.01	-0.09	0.12	...	0.18	...
UZ Cen	-0.02	-0.08	-0.07	-0.05	-0.22	0.10	-0.07	0.09	0.05	-0.06	-0.07	0.13	0.01	...
Y Car	0.02	-0.11	-0.02	-0.10	-0.30	0.17	0.08	0.09	0.10	-0.10	0.08	0.10	0.08	...
AX Vel	-0.05	-0.14	-0.11	0.05	-0.30	0.08	-0.25	0.13	0.04	-0.14	-0.02	...	-0.02	...
V701 Car	0.07	-0.06	0.08	-0.03	-0.10	0.23	0.10	0.01	0.11	-0.01	0.01	...	0.07	...
GZ Car	0.00	-0.11	-0.02	0.07	...	0.09	0.04	0.11	0.06	-0.25	-0.05	...	0.08	-0.05
BQ Ser	-0.04	-0.11	-0.04	0.06	-0.29	0.12	-0.10	0.20	-0.02	-0.34	0.12	0.27	0.10	0.20
V1210 Cen	0.08	-0.03	0.04	0.05	-0.17	0.25	0.01	0.18	0.02	-0.22	0.06	...	0.17	...
V458 Sct	0.09	0.09	0.11	0.13	-0.16	0.21	-0.13	0.17	0.03	-0.20	0.05	0.11	0.11	...
EW Sct	0.04	-0.07	0.00	0.04	-0.27	0.20	0.01	0.25	-0.02	-0.12	0.13	0.26	0.11	...
V367 Sct	0.05	-0.12	0.11	0.09	0.32	0.17	-0.07	0.17	0.00	-0.21	0.08	...	0.23	...

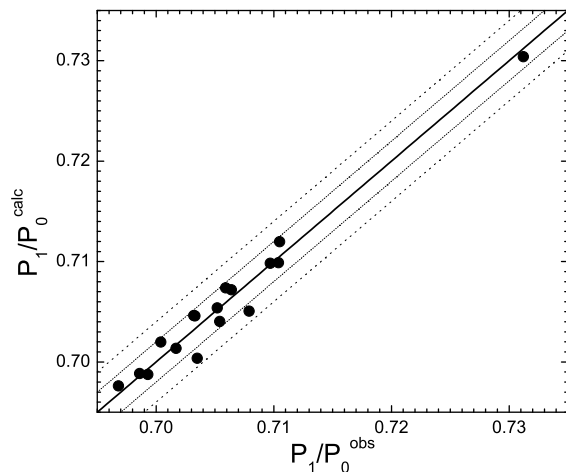


Figure 1: The comparison between the calculated P_1/P_0 ratios and P_1/P_0 ratios obtained from the observations. The ranges of error for σ and 2σ are marked with *dotted lines*.

of the α -elements, and the iron-peak elements. Though the abundances of oxygen and some other elements are about 9 dex, the iron-peak elements contribute most to the opacity.

It is known that the electron scattering plays an important role in the light energy absorption in the extended atmospheres of supergiants; therefore, the opacity depends on the electron density. The iron-peak elements, which are mainly in ionised form, supply free electrons. Thus, the period ratio P_1/P_0 tends to show greater sensitivity to the iron-peak elements, and lower or even zero sensitivity to other elements.

Our analysis of the final model has fully confirmed the validity of the initial assumptions. As expected, oxygen along with a number of other elements was not factored in the further analysis. Two α -elements, namely Ca and Si, showed a rather good correlation. But the greatest sensitivity of the relation was found for several iron-peak elements, such as Cr, Mn, Fe, Co and Ni. Given the crucial importance of the physical value, such as $[Fe/H]$, we constructed an empirical relation for P_1/P_0 , P_0 and $[Fe/H]$. The resulted relationship is as follows:

$$P_1/P_0 = 0.719 - 0.024 \log P_0 - 0.041 [Fe/H] \pm 0.002 \pm 0.003 \pm 0.004.$$

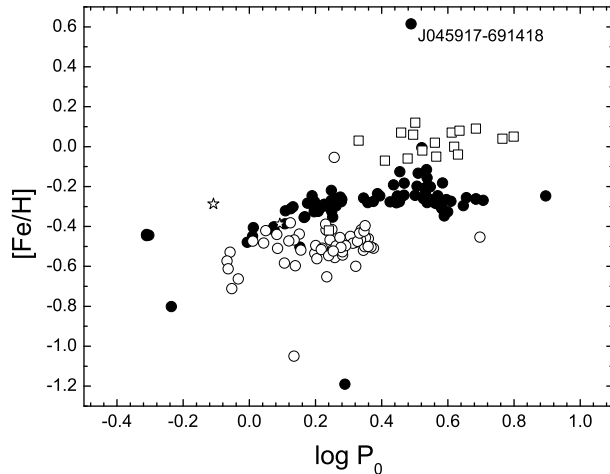


Figure 2: Dependence of the $[Fe/H]$ abundance on $\log P_0$. *Open squares* – the Galactic beat Cepheids (program stars); *open stars* – the P_1/P_0 Cepheids of the Galactic bulge; *full circles* – the bimodal Cepheids of the LMC and *open circles* – those of the SMC.

The results of a comparison of the calculated P_1/P_0 values with the data obtained from the photometric observations are presented in Fig.1. The standard deviation is ± 0.002 ; the correlation coefficient R^2 is 0.97.

5. Confirmation and discussion

There are a small number of beat Cepheids in our Galaxy for a full confirmation of the derived relationship. The situation is better for the Magellanic Clouds. We have applied data from several sources: the EROS-2 database by Marquette et al. (2009), as well as the OGLE-III survey results by Soszyński et al. (2008) and Soszyński et al. (2010). It helped us to gather data for more than 90 beat Cepheids pulsating in the P_1/P_0 modes in the LMC and more than 60 in the SMC.

Using our relation, we estimated metallicities for the above-mentioned samples of stars. Figures 2 and 3 show the $[Fe/H]$ sensitivity to $\log P_0$ and P_1/P_0 , respectively. As can be seen, there is a pronounced trend in Fig. 3. The Cepheid J045917-691418, whose data are shown in Fig. 3, drew our attention with its unusually high metallicity of 0.61 dex. Such a high value is anomalous not only for the Magellanic Clouds Cepheids, but also for Galactic pulsators.

According to modern theoretical calculations, the evolutionary tracks of high metallicity stars do not reach the instability strip. Therefore, based on theoretical models, it is possible to assume that Cepheids with such a high metallicity do not exist.

To examine the case further, we focused our atten-

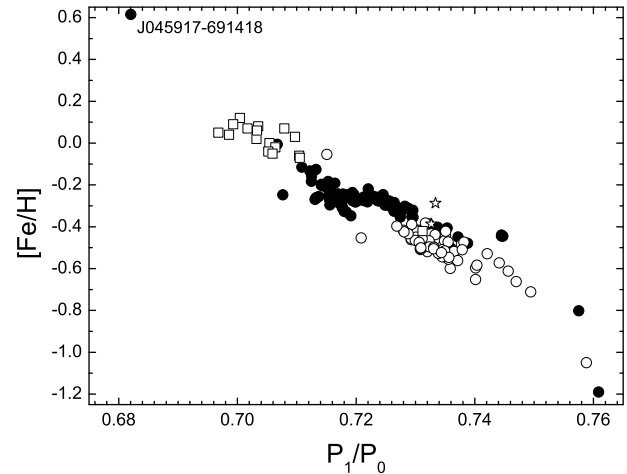


Figure 3: Dependence $[Fe/H]$ vs. P_1/P_0 ratio. Symbols are the same as in Fig. 2.

tion on the anomalous star. Such a subnormal value of P_1/P_0 for J045917-691418 was taken from the EROS-2 database. We searched for alternative data on that Cepheid and found an object with the same coordinates in the OGLE database. In the OGLE database that Cepheid was identified as a fundamental mode pulsator with a note that it might be a binary star with a first-overtone pulsator companion. That star should be restudied more thoroughly, but it requires new observations.

We can only assume that both study groups can be right in their definitions. The fact is that when a star reaches the instability strip, its mode of pulsation is quite unstable, and that can result in a very rapid change in pulsation periods. Since both the OGLE and EROS-2 observations are time-separated, it is likely that we face a similar situation. Thus, J045917-691418 is of great interest for further research.

We also constructed a metallicity distribution function for the Magellanic Clouds projected on the celestial sphere (see Fig. 4). A few regions with increased metallicity can be seen in the centre of the LMC projection. Although usually the distribution corresponds to the nature of irregular galaxies, no specific structures or formations are observed in the projection.

The average metallicities of the Magellanic Clouds were obtained independently: -0.30 dex for the LMC and -0.49 dex for the SMC. The average metallicity for the LMC is in good agreement with standard values obtained from spectral studies of B-supergiants or F-K supergiants. The average metallicity for the SMC is somewhat higher than common values obtained by other authors, but it is in very good agreement with the value obtained by Chekhonadskikh (2012) who used classical Cepheids in his study.

There were two double-mode P_1/P_0 Cepheids among a sample of new classical Cepheids discovered

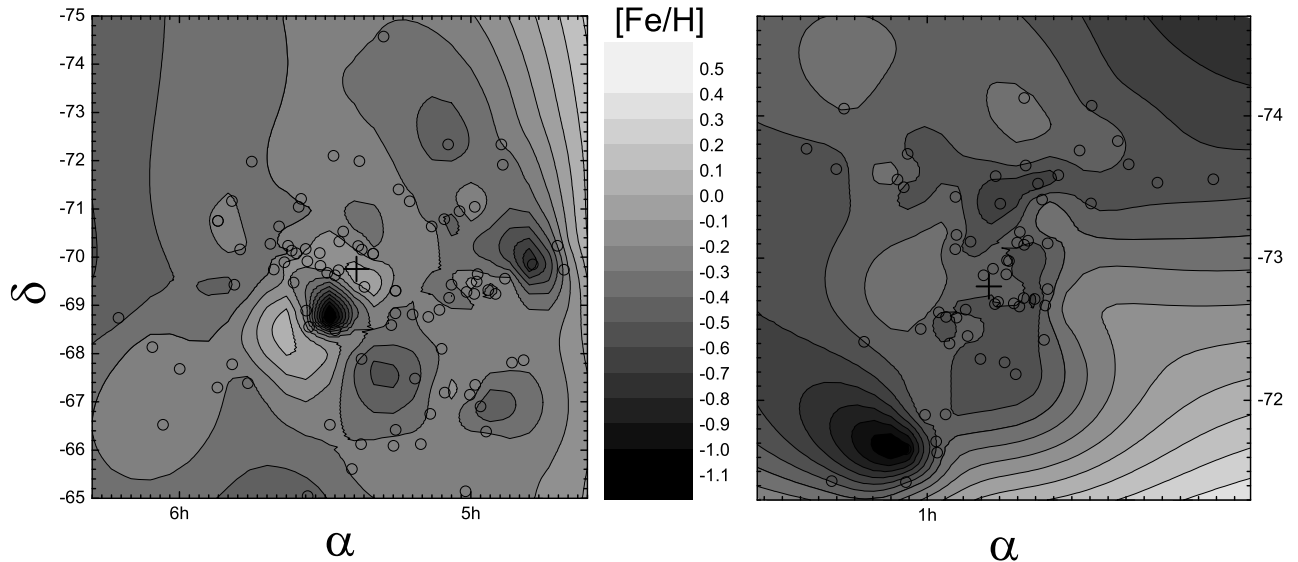


Figure 4: The $[\text{Fe}/\text{H}]$ distribution in the LMC (left) and SMC (right) projected on the celestial sphere. *Open circles*: positions of the stars; *bold crosses*: positions of the galactic centres.

by Soszynski et al. (2011) in the Galactic bulge. We have also derived $[\text{Fe}/\text{H}]$ for those Cepheids: -0.39 dex for OGLE-BLG-CEP-03 and -0.29 dex for OGLE-BLG CEP-21. The estimates are also given in Fig. 2 and Fig. 3.

6. Conclusions

New, accurate, and homogeneous abundances for a number of chemical elements, as well as physical atmospheric parameters, were determined for a large number of Galactic bimodal Cepheids using high-resolution and high S/N echelle spectra. The new abundances obtained and fundamental parameters are in good agreement with the results of other analyses in the literature.

A statistical analysis of the P_1/P_0 - $A(EI)$ correlation was conducted. The observed period ratios for the program stars exhibited a strong dependence on the abundances of several chemical elements. A new, more accurate P_1/P_0 - $[\text{Fe}/\text{H}]$ relation was suggested.

Based on the newly suggested relation, alternative $[\text{Fe}/\text{H}]$ values were found for a large number of beat Cepheids in the Magellanic Clouds, and thereby independent average metallicities for the Magellanic Clouds were obtained. The metallicity distribution function for the Magellanic Clouds projected on the celestial sphere was constructed for the first time.

The $[\text{Fe}/\text{H}]$ values for two new double-mode P_1/P_0 Cepheids in the Galactic bulge were estimated for the first time.

Acknowledgements. FAC gratefully acknowledges financial support for this work from the Swiss National Science Foundation, project SCOPES No. IZ73Z0-152485.

References

- Andrievsky S.M., Kovtyukh V.V., Luck R.E., et al.: 2002, *A&A*, **381**, 32.
- Chekhonadskikh F.A.: 2012, *KPCB*, **28/3**, 128.
- Galazutdinov G.A.: 1992, *Prepr. SAO RAS*, **92**, 2.
- Grevesse N., Noels A. & Sauval J.: 1996, *ASP Conf. Ser.*, **99**, 117.
- Kovtyukh V.V.: 2007, *MNRAS*, **378**, 617.
- Kovtyukh V.V. & Andrievsky S.M.: 1999, *A&A*, **351**, 597.
- Kovtyukh V.V., Gorlova N.I. & Hillen M.: 2012, *OAP*, **25/1**, 52.
- Marquette J.B., Beaulieu J.P., Buchler J.R., et al.: 2009, *A&A*, **495**, 249.
- Soszyński I., Poleski R., Udalski A., et al.: 2008, *Acta Astron.*, **58**, 163.
- Soszyński I., Poleski R., Udalski A., et al.: 2010, *Acta Astron.*, **60**, 17.
- Soszyński I., Udalski A., Pietrukowicz P., et al.: 2011, *Acta Astron.*, **61**, 285.
- Sziládi K., Vinkó J., Poretti E., et al.: 2007, *A&A*, **473**, 579.
- Udalski A., Szymański M.K., Soszyński I. & Poleski R.: 2008, *Acta Astron.*, **58**, 69.